CHINESE OPTICS LETTERS

Vol. 19, No. 12 | December 2021

10 Gb/s free space optical interconnect with broadcasting capability enabled by a silicon integrated optical phased array

Quan You (尤 全)[1,2], Daigao Chen (陈代高)[1], Xi Xiao (肖 希)[1,2*], and Shaohua Yu (余少华)[1,2]

[1] National Information Optoelectronics Innovation Center, China Information Communication Technologies Group Corporation (CICT), Wuhan 430074, China

[2] State Key Laboratory of Optical Communication Technologies and Networks, China Information Communication Technologies Group Corporation (CICT), Wuhan 430074, China

*Corresponding author: xiaoxi@noeic.com

Received July 28, 2021 | Accepted October 14, 2021 | Posted Online November 3, 2021

We have proposed and experimentally demonstrated a reconfigurable free space optical interconnect with broadcasting capability based on an eight-channel silicon integrated optical phased array. By using the silicon integrated beam steering and broadcasting device, 10 Gb/s on–off keying data is transmitted over 15 cm in free space for up to three receivers located in three different cards. The experimental results show that the optical phased array can be used with broadcasting capability provided to multi-receivers in the card to card optical interconnects, which can significantly reduce device size, system complexity, and total costs.

Keywords: optical phased array; optical interconnect; card to card transmission.

DOI: 10.3788/COL202119.120602

1. Introduction

Optical interconnect technology has been widely used in card to card (CtC) communications and highly demanded in the servers and storage in data centers. Limited by the low speed and narrow bandwidth, traditional electrical interconnects could not be the best solution for the future service in high-capacity transmission systems. The optical wireless communications without electro-optical transformation can provide almost unlimited bandwidth connectivity to users with sample transceivers, low cost, and integrated system, which has attracted great attention in the field of free space optical interconnects[1–4]. The transmission distance in a CtC transmission system is about 10 cm to 100 cm in free space generally[5,6]. In a reconfigurable free space CtC communication system, a spatial light modulator (SLM) such as a micro-electro-mechanical systems (MEMS) mirror[7] or liquid crystal on silicon (LCOS) device[8] is necessary to steer the optical beams carried with high data rate signals to the receivers, which are located in different cards. By applying corresponding voltage on the MEMS mirror or corresponding phase distribution onto the LCOS, the optical beam can be steered with a desired reflection angle. A MEMS-based reconfigurable free space optical interconnect was demonstrated in Ref. [9], where a 30 Gb/s optical signal was transmitted over 30 cm free space distance with bit error rate (BER) lower than 10^{-6}. A LCOS-based reconfigurable free space optical interconnect was demonstrated in Ref. [10], and the measured results showed that a 1.25 Gb/s optical signal was received with BER lower than 10^{-12} in a short distance transmission. However, these two schemes can only steer the optical beam pointing to one position at a time. In order to realize card to multi-card (CtMC) free space transmission, also called optical broadcasting, a MEMS-based reconfigurable optical interconnect was proposed in Ref. [11], where a 10 Gb/s optical signal was broadcast to three receiver cards with transmission distance of 30 cm in free space. Also an opto-very-large-scale integration-processor-based reconfigurable optical interconnect was proposed in Ref. [12], where a 2.5 Gb/s data broadcast for two receiver cards with a short transmission distance was reported. The steering and broadcasting functions between the transmitter and receiver cards were realized by applying switching and multicasting phase holograms into the processors.

The silicon photonic optical phased array (OPA) is also used in high-speed point to point free space communications[13,14], as it can provide agile and precise optical beam steering without any moving parts. Based on the silicon on insulator (SOI) platform and existing complementary metal oxide semiconductor (CMOS) technologies, silicon integrated photonic circuits used in CtC optical interconnects will significantly reduce the module size and overall cost[15–18]. In this paper, we experimentally demonstrated an eight-channel silicon integrated OPA-based

optical interconnect with broadcasting capability in free space transmission. Based on the silicon integrated beam steering and broadcasting device, a 10 Gb/s on–off keying (OOK) data is transmitted over 15 cm in free space for up to three receivers located in three different cards. To the best of our knowledge, this is the first OPA-based reconfigurable CtMC optical interconnect architecture with high-speed transmission.

2. Operation Principle

Figure 1 shows the architecture of the reconfigurable free space optical interconnect used in the field of CtC and CtMC. An optical interconnect module always includes a transmitter and a receiver integrated on a printed circuit board (PCB). The optical wavelength carried with a high data rate signal is generated by the transmitter and modulated by an OPA into optical beam forms. The optical beam is ejected into free space with scanning angles when the OPA is used for CtC transmission or separated into multiple beams when it is used for CtMC transmission. After transmitting a short distance in free space, photodiodes (PDs) located on the receiver cards are used to detect the optical signal. The multiple receivers located in different cards are served by the same transmitter and all the receivers share the same optoelectronic components like laser source and modulators.

In our reconfigurable optical broadcasting system, an eight-channel silicon integrated phased array is set at the transmitter card. The integrated silicon OPA here is fabricated on an SOI wafer with a 220 nm thick silicon layer and a 3 μm thick box layer. The width of one channel grating is 4 μm, and the channel space is 5 μm. The etching depth of the grating area is 70 nm. The gratings have a pitch of 630 nm with a duty cycle of 0.55. The device is fabricated by the commercial CMOS platform, and the whole wafer is cladded by a SiO_2 upper-cladding. In this work, we use a TiN heater to tune the optical phase. The TiN heaters are modulated by a multi-channel DC power source. The integrated silicon OPA can steer the output beam into different angles or separate the output beam into several equal ones by operating the optical phase of each channel. Different power combinations for the phase arms can generate different beam propagation cases. Figure 2(a) shows the optical microscope image of the proposed eight-channel phased array; its size is 0.7 mm × 1.7 mm. Figure 2(b) shows the photo of the wire-bonded phased array on the PCB. Figure 2(c) exhibits the schematic diagram of the channel grating design in the proposed OPA. Here, we used the edge coupling method to guide the optical beam out from a standard single mode fiber (SSMF) into the waveguide of the OPA. Different from grating coupling, which is an out-of-plane coupling, the edge coupling is a kind of in-plane coupling and more appropriate for integrating on a PCB to realize free space optical transmission. Also, the edge coupler will introduce lower polarization dependent loss and lower wavelength sensitivity, which makes the free space optical interconnect more stable[19]. At the output side of the OPA chip, the optical beam is ejected into free space from the grating arrays.

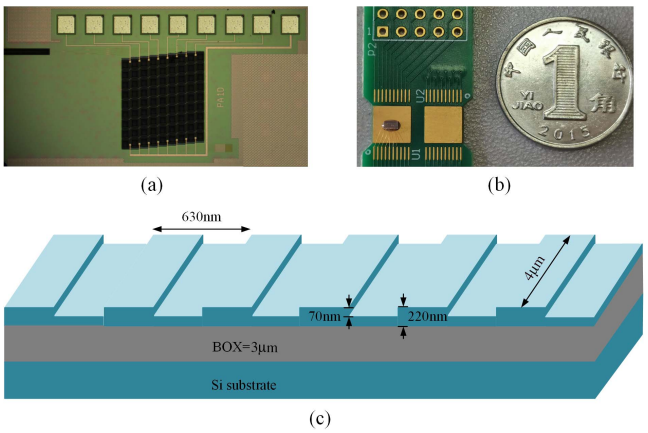

Fig. 2. (a) Microscope image of the proposed OPA. (b) Photo of the wire-bonded OPA on the PCB. (c) Schematic diagram of the channel grating in the proposed OPA.

We use an infrared CCD (OPHIR Photonics) at the output side of the OPA to observe near-field optical beam distribution. When the OPA is used for CtC transmission, the output beam has only one spot, as shown in Fig. 3(a). The divergence angle of the output beam is 2.1° × 3.6°. When the OPA is used for card to two-cards (Ct2C) and card to three-cards (Ct3C) transmissions, the optical beam is separated into two and three similar spots, as seen in Figs. 3(b) and 3(c), and the angles between adjacent optical beams are about 28° and 14°, respectively. It is worth noting that we raised the launch power into the OPA with 3 dB and 4.8 dB gain for these two broadcasting schemes. Therefore, at least three receivers located in three cards can receive the broadcasting signal simultaneously based on our fabricated silicon integrated OPA. Of course, when we offer different voltage

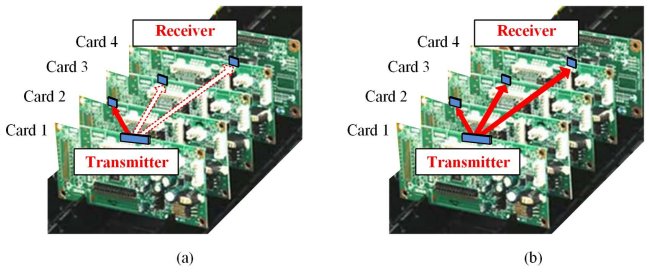

Fig. 1. Architecture of the proposed reconfigurable optical interconnect used in the field of (a) card to card and (b) card to multi-card.

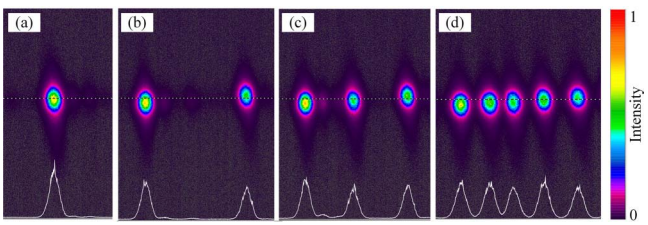

Fig. 3. Optical beam detected by an infrared CCD: (a) one spot; (b) two similar spots; (c) three similar spots; (d) five similar spots.

combinations at the transmitter card, different beam propagation was generated. The number of similar optical beams was up to five, as seen in Fig. 3(d). Based on this operation, the reconfigurable optical broadcasting service can be realized.

3. Experiments and Results

We first measured the optical power losses at different transmission distances when the OPA provided CtC service with a 0° steering angle. By using a free space optical power meter (Coherent, FieldMaxII-Top), which is set at the focal point of a lens with a focal length of 10 mm, the measured power losses are 10.1 dB, 10.6 dB, 10.9 dB, 11.1 dB, and 11.5 dB after 11 cm, 12 cm, 13 cm, 14 cm, and 15 cm transmission, as seen in Fig. 4(a). The optical power loss raised with the increasing of transmission distance; it is mainly because the beam footprints are larger after longer distance transmission, which reduces the value of optical power collected by the power meter. The end-to-end loss of the OPA device is 8 dB (including coupling loss between input fiber and OPA device) when transmission distance is 0 cm. Then, we measured the power losses versus different steering angles when the transmission distance is 15 cm. The measured optical power losses are 11.5 dB, 11.6 dB, and 11.9 dB when the steering angle is 0°, 7°, and −7° (CtC #1, #2, and #3), as shown in Fig. 4(b). Figure 4(b) also exhibits the measured optical power losses when the OPA provides CtMC service with 15 cm transmission distance. The measured optical power losses are

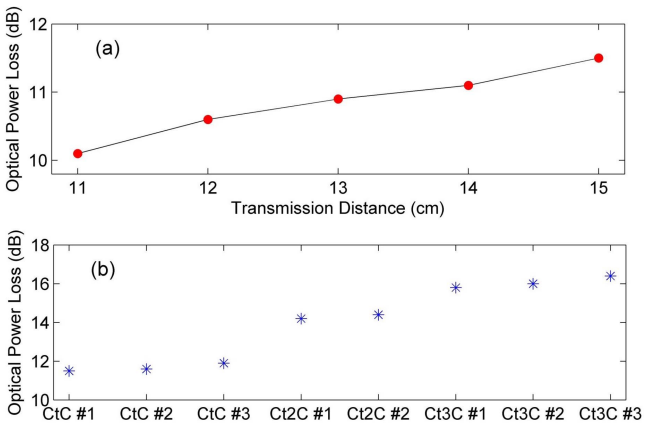

Fig. 4. (a) Measured optical power loss versus different transmission distance with 0° steering angle. (b) Measured optical power loss versus different transmission schemes with 15 cm transmission distance.

14.2 dB, 14.4 dB, 15.8 dB, 16 dB, and 16.4 dB when the OPA provides Ct2C (#1 and #2) and Ct3C (#1, #2, and #3) service, respectively. The maximal fluctuation of the optical power loss for these three schemes (CtC, Ct2C, and Ct3C) is 0.9 dB when the splitting losses (3 dB for two beams and 4.8 dB for three beams) are not considered in the calculation.

In order to verify the directional stability of beams emitted by the OPA, we measured the centroid position of the output beam when the OPA provided CtC transmission. Here, we take the infrared CCD instead of the free space optical power meter to observe the centroid position of the output beam with 5 min spacing, and the results in 1 h measurement are shown in Table 1. The original position was measured at the fifth minute, and its coordinate was set as (0, 0). It can be seen that the centroid position of the spot was slightly moved at the room temperature of 20°C. The Gaussian beam waist at the CCD plane was $\omega_x = 0.203$ mm in the X direction and $\omega_y = 0.193$ mm in the Y direction, respectively. The fluctuation of received optical power caused by the instability of the output beam can be obtained by calculating the coupling loss of the Gaussian beams with displacement mismatch Δx in the X direction and Δy in the Y direction. Here, we chose the maximal $\Delta x = 0.005$ mm and maximal $\Delta y = 0.006$ mm from Table 1, where the maximal coupling loss was calculated to be 0.0068 dB theoretically. The fluctuation of the received optical power at the PD plane caused by the instability of the output beam can be ignored, which suggests that the proposed free space optical interconnect has good long-term stability for deploying in laboratory scenarios.

As shown in Fig. 5, we conduct an experiment to verify the effectiveness of the designed reconfigurable CtMC optical interconnect. First, a pseudo random binary sequence (PRBS) with length of $2^{17} - 1$ is generated by a bit error tester (BERT), which runs at 10 Gb/s. Then, the signal is modulated by a Mach–Zehnder modulator (MZM), which is amplified by an electrical driver. The optical signal is generated by an Agilent external cavity laser at the region around 1545 nm and then amplified by an erbium-doped optical fiber amplifier (EDFA). A polarization controller (PC) is introduced here to confirm the best polarization situation of the optical beam coupled into the eight-channel phased array integrated circuit through an SSMF. After being modulated by the OPA, the optical signal is transmitted in free space for a short distance and arrives at the receiver side. Since the optical beams propagated from the OPA surface and injected into the free space, their diameter expands as the transmission distance increases, so a focusing lens with a focal length of 10 mm is used to collect the divergence beam onto the

Table 1. Measured Centroid Coordinates of the Output Beams with 5 min Spacing in 1 h.

Time (min)	5	10	15	20	25	30	35	40	45	50	55	60
X (mm)	0	0.001	−0.004	−0.001	−0.002	0.005	0.001	−0.004	0	−0.004	−0.002	−0.004
Y (mm)	0	−0.006	−0.001	0.002	−0.001	−0.001	−0.001	−0.004	−0.002	0.001	−0.005	−0.003

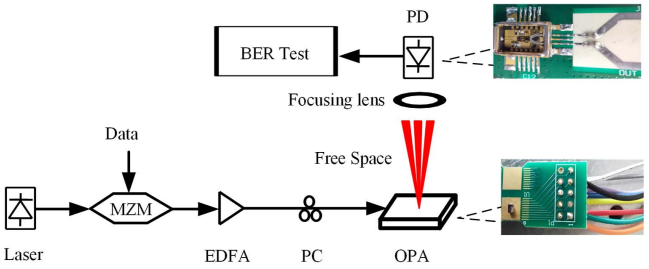

Fig. 5. Experiment setup of the optical broadcasting system with the proposed OPA. MZM, Mach–Zehnder modulator; EDFA, erbium-doped fiber amplifier; PC, polarization controller; PD, photodiode; OPA, optical phased array.

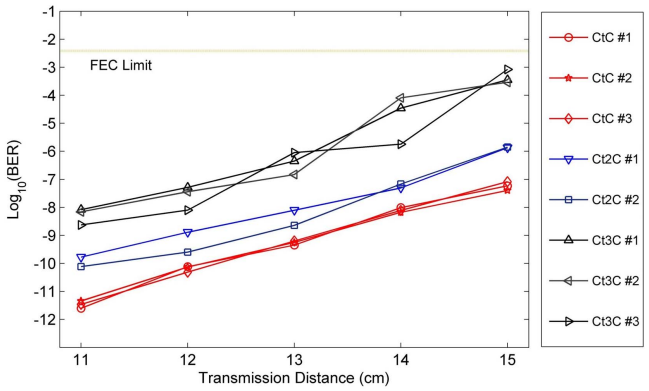

Fig. 6. BER value of the 10 Gb/s OOK signal versus transmission distance for different transmission schemes.

PD surface. After detection, the performance of the electrical signal is characterized by the BERT.

In order to verify the steering and broadcasting functions of the optical interconnect based on the proposed experimental setup, we measured the BER performance of the signal as a function of transmission distance for the different transmission schemes, as shown in Fig. 6. The optical powers launched into the OPA device are amplified to 10 dBm by the EDFA for all three transmission schemes. Since the intensity of the optical beams is almost the same for different transmission schemes, similar BER performances are achieved. The achieved BER values are all below the 7% forward error correction (FEC) limit at the BER value of 3.8×10^{-3}. The measured results indicate that the proposed reconfigurable CtMC optical interconnect with high validity and feasibility can be used in future high-capacity optical wireless communications.

In our experiment, the performance of the optical broadcasting system is limited by the received optical power at the PD surface, which results in a few receiver cards getting the broadcasting signal at the same time. To solve this issue, a lower beam divergence and higher coupler efficiency OPA is needed at the transmitter side[20,21]. At the receiver side, a more aligned optical receiver system can focus more optical power on the PD surface. After optimizing the design of the OPA device and optical link, the transmission distance and number of receiver cards of the broadcasting system will be improved.

4. Conclusions

We have proposed and experimentally demonstrated a reconfigurable optical CtMC interconnect by using an eight-channel OPA. Based on the silicon integrated optical beam steering and broadcasting device, a 10 Gb/s optical signal is transmitted for up to three cards with BER $< 3.8 \times 10^{-3}$. Obviously, the silicon integrated OPA is suitable for future CtMC interconnects. By optimizing the design of the silicon integrated device and employing a more aligned optical system, the number of the receiver cards accessed in the optical interconnects can be developed.

Acknowledgement

This work was supported by the National Key Research and Development Program of China (No. 2019YFB2203203).

References

1. M. A. Taubenblatt, "Optical interconnects for high-performance computing," J. Lightwave Technol. **30**, 448 (2012).
2. X. Zhou, H. Liu, and R. Urata, "Datacenter optics: requirements, technologies, and trends," Chin. Opt. Lett. **15**, 120008 (2017).
3. Q. Kong, Y. Zhan, and P. Wan, "Hybrid OCS/OBS interconnect in intra-data-center network," Chin. Opt. Lett. **17**, 080605 (2019).
4. G. Song, J. Zou, and J. He, "Ultra-compact silicon-arrayed waveguide grating routers for optical interconnect systems," Chin. Opt. Lett. **15**, 030603 (2017).
5. Y. Li, E. Towe, and M. W. Haney, "Scanning the issue-special issue on optical interconnections for digital systems," Proc. IEEE **88**, 723 (2000).
6. H. Cho, P. Kapur, and K. C. Saraswat, "Power comparison between high-speed electrical and optical interconnects for inter-chip communication," J. Lightwave Technol. **22**, 2021 (2004).
7. S. Li, Z. Wan, J. Xu, S. Zhong, and Y. Wu, "Wavelength-selective switch based on a high fill-factor micromirror array," Chin. Opt. Lett. **9**, 090601 (2011).
8. F. Pan, L. Kong, X. Yang, Y. Ai, and Y. Zhou, "Dual beam deflection of liquid crystal optical phased array," Chin. Opt. Lett. **10**, S20502 (2012).
9. C. J. Henderson, D. Gil-Leyva, and T. D. Wilkinson, "Free space adaptive optical interconnect at 1.25 Gb/s, with beam steering using a ferroelectric liquid-crystal SLM," J. Lightwave Technol. **24**, 1989 (2006).
10. K. Wang, A. Nirmalathas, C. Lim, E. Skafidas, and K. Alameh, "High-speed reconfigurable free-space card-to-card optical interconnects," Photonics J. IEEE. **4**, 1407 (2012).
11. K. Wang, A. Nirmalathas, C. Lim, E. Skafidas, and K. Alameh, "High-speed free-space based reconfigurable card-to-card optical interconnects with broadcast capability," Opt. Express **21**, 15395 (2013).
12. M. Aljada, K. E. Alameh, Y.-T. Lee, and I.-S. Chung, "High-speed (2.5Gbps) reconfigurable inter-chip optical interconnects using opto-vlsi processors," Opt. Lett. **14**, 6823 (2006).
13. K. Wang, A. Nirmalathas, C. Lim, E. Wong, K. Alameh, H. Li, and E. Skafidas, "High-speed indoor optical wireless communication system employing a silicon integrated photonic circuit," Opt. Lett. **43**, 3132 (2018).
14. H.-W. Rhee, J.-B. You, H. Yoon, K. Han, M. Kim, B. Goo Lee, S.-C. Kim, and H.-H. Park, "32 Gbps data transmission with 2D beam-steering using a silicon optical phased array," IEEE Photonics Technol. Lett. **32**, 843 (2020).
15. J. K. Doylend, M. J. R. Heck, J. T. Bovington, J. D. Peters, L. A. Coldren, and J. E. Bowers, "Free-space beam steering in two dimensions using a silicon optical phased array," in *Optical Fiber Communication Conference* (2012), paper OM2J.1.
16. D. Kwong, A. Hosseini, J. Covey, Y. Zhang, X. Xu, H. Subbaraman, and R. T. Chen, "On-chip silicon optical phased array for two-dimensional beam steering," Opt. Lett. **39**, 941 (2014).
17. K. Van Acoleyen, H. Rogier, and R. Baets, "Two-dimensional optical phased array antenna on silicon-on-insulator," Opt. Lett. **18**, 13655 (2010).

18. K. Liu, Q. Wei, Y. Huang, X. Duan, Q. Wang, X. Ren, and S. Cai, "Integrated optoelectronic chip pair for transmitting and receiving optical signals simultaneously," Chin. Opt. Lett. **17**, 041301 (2019).
19. J. He, T. Dong, and Y. Xu, "Review of photonic integrated optical phased arrays for space optical communication," IEEE Access **8**, 188284 (2020).
20. H.-W. Rhee, M. Kim, J.-B. You, and H.-H. Park, "High-speed data transmission system using silicon-based optical phased array," Proc. SPIE **11286**, 112861A (2020).
21. M. Zadka, Y.-C. Chang, A. Mohanty, C. T. Phare, S. P. Roberts, and M. Lipson, "On-chip platform for a phased array with minimal beam divergence and wide field-of-view," Opt. Express **26**, 2528 (2018).